DEEPENING OBSERVED SINCE THE 1950s IN MID-DEPTH OCEAN ISOPYCNALS DUE TO GLOBAL WARMING

S. Hakkinen, Cryospheric Sciences, NASA GSFC, P. B. Rhines, UW,
D. L. Worthen, Cryospheric Sciences, WTS/GSFC

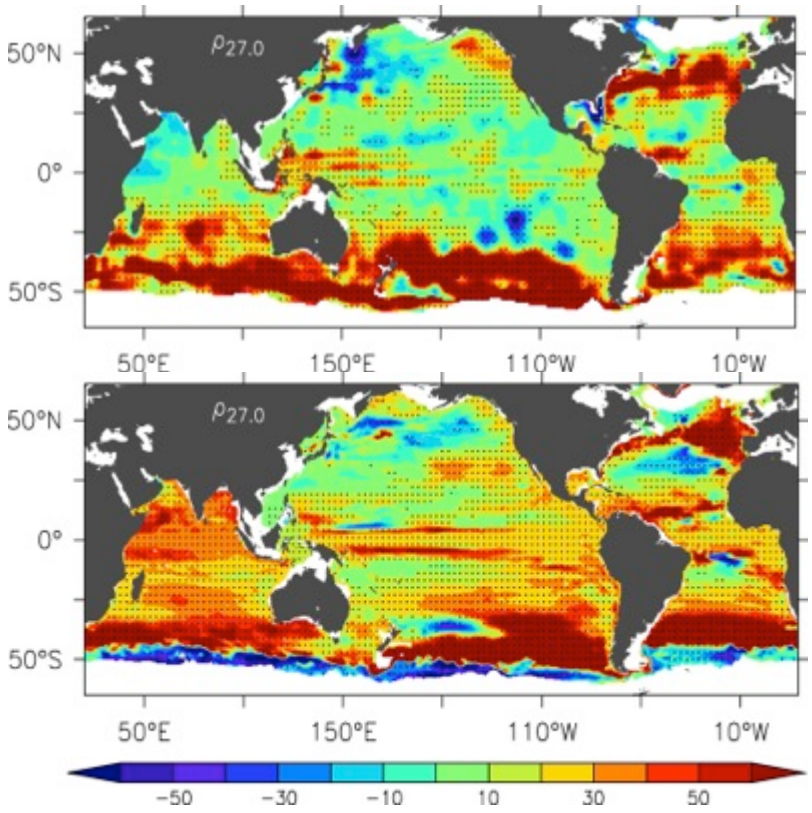

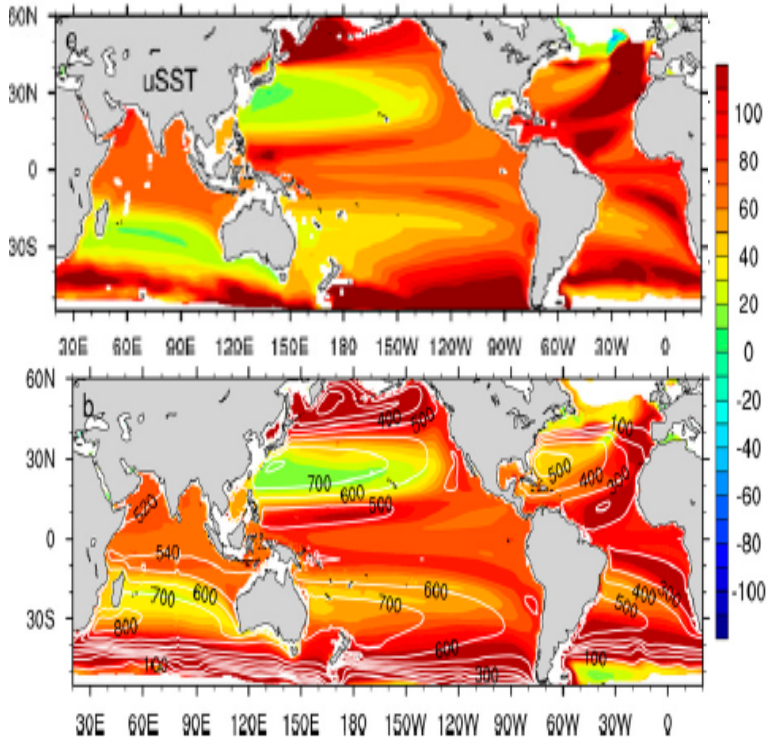

Besides surface warming, global warming also has a subsurface effect of a strong deepening of the mid-thermocline isopycnals. This is a result of heat entering via subduction in high-latitude ventilation regions of subtropical mode waters and spreading laterally.

Name: Sirpa Hakkinen, Cryospheric Sciences, NASA GSFC
E-mail: Sirpa.Hakkinen@nasa.gov
Phone: 301-614-5712

References:

This research '**Warming of the global ocean: spatial structure and water-mass trends**' will appear in *Journal of Climate* 2016.

Data Sources: UK Met Office objectively analyzed ocean observations (EN4) (1948-) (1x1 deg), ocean state estimate by SODA : Ocean state analysis (0.5x0.5 deg) (1955-2011)

Technical Description of Figures:

Graphic 1: Isopycnal deepening is near maximum at the 27.0 density surface, its deepening for 1955-2011 is shown for EN4 (top, left) & SODA (bottom, left) [meters/50years]. Stippling denotes 95% significance. On the right, the change in the depth of the 26.8 density surface [meters] from 1976-2000 to 2076-2100 based on fixed uniform SST forcing (from CMIP5) of OGCM +climatology (top) and from CMIP5 results (bottom); from Wang et al., JClimate 2015. Note the similar regions of activity especially in the Southern Hemisphere, north of the Antarctic Circumpolar Current, where at these density ranges increased amount of Subantarctic Mode Water slides northward under surface waters displacing Antarctic Intermediate Water.

Scientific significance, societal relevance, and relationships to future missions: This mid-depth isopycnal deepening is a direct result of warming climate and specifically how warming climate influences formation of deeper water masses, where subtropical mode formation increases while subpolar mode water formation decreases. On multi-decadal scales is expected to be the primary contributor to sinking of subtropical mode water isopycnals, however additional dynamic impacts from very low-frequency changes in atmospheric modes, e.g. NAO and SAM, are likely present in our data.

Assessing EO-1 and Landsat instrument capabilities for mapping Great Lakes ice

Christopher J. Crawford, Cryospheric Sciences, NASA GSFC and ESSIC, Petya K. Campbell, Biospheric Sciences, NASA GSFC and UMBC,
Elizabeth M. Middleton, Biospheric Sciences, NASA GSFC, Dorothy K. Hall, Cryospheric Sciences, NASA GSFC and ESSIC,
Milton G. Hom, Biospheric Sciences, NASA GSFC and SSAI, Karl F. Huemmrich, Biospheric Sciences, NASA GSFC and UMBC,
and David R. Landis, Biospheric Sciences, NASA GSFC and GST, Inc.

Only ice surface retrieval results for the Lake Superior Apostle Islands channel are shown (grey box above)

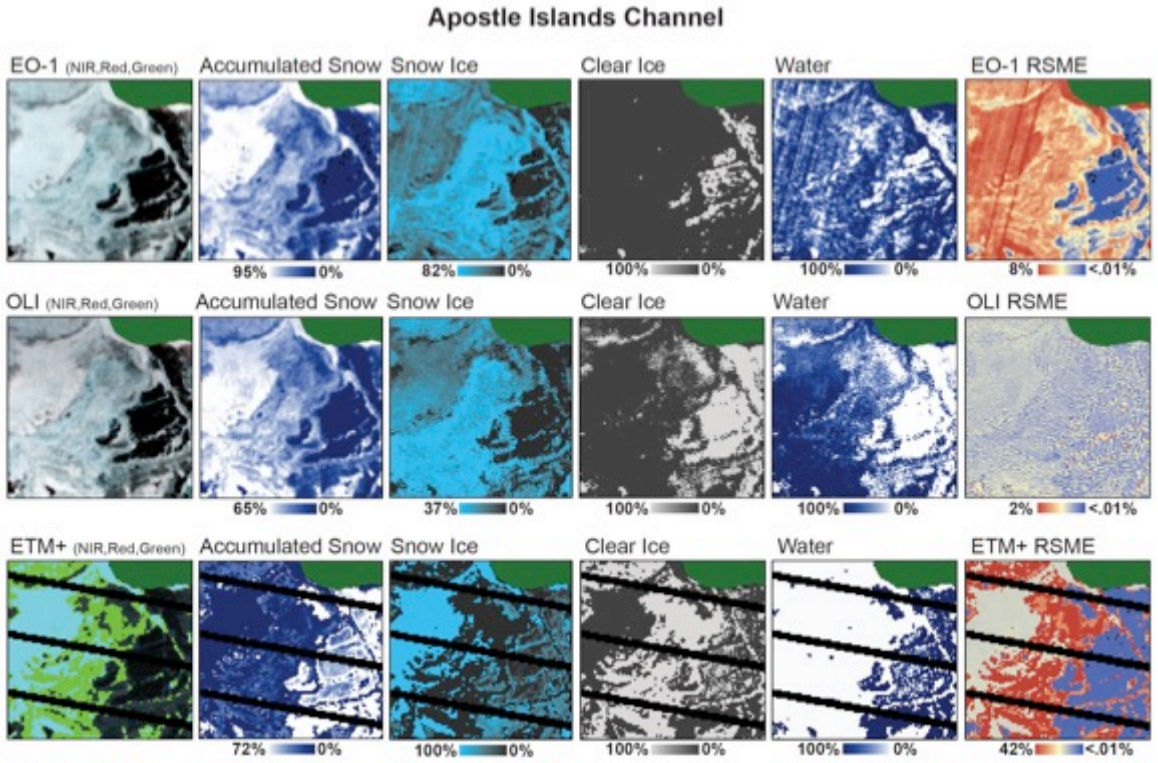

We used ground-based spectroscopic measurements to assess how spectral resolution constrains instrument capabilities for retrieving optical snow, ice, and water properties from space.

Name: Christopher J. Crawford, Cryospheric Sciences, NASA GSFC and Earth System Science Interdisciplinary Center at University of Maryland
E-mail: christopher.j.crawford@nasa.gov
Phone: 301-614-6486

References:

Crawford, C.J., P.K. Campbell, E.M. Middleton, D.K. Hall, M.G. Hom, K.F. Huemmrich, and D.R. Landis (in press) Retrieval of Lake Superior Ice Surfaces using EO-1 Hyperion, Landsat ETM+, and Landsat OLI. Proceedings from the *23rd IAHR International Symposium on Ice*

Data Sources: 1) **NASA EO-1** and **Landsat** Earth observations; 2) ground-based spectroscopic measurements acquired with a **NASA/GSFC Code 610 ASD field spectrometer**. Acknowledgments: Christopher J. Crawford was funded through a NASA Postdoctoral Program Fellowship (NNH06CC03B) appointment at the GSFC administered by Oak Ridge Associated Universities, the NASA Terrestrial Hydrology Program, and University of Maryland, College Park/NASA Cooperative Agreement (NNX12AD03A). We thank George A. Leshkevich at NOAA GLERL for his guidance and assistance in collecting ice measurements on Lake Michigan. We thank Shawn Heckman/Madeline Island Ferry Line for ice measurement assistance on Lake Superior.

Technical Description of Figures:

Graphic 1: Atmospherically corrected EO-1 Hyperion, Landsat ETM+, and Landsat OLI images for the February 24, 27, and 28, 2015 study period. A time series of EO-1 acquisitions was scheduled during January through March 2015 over a Lake Superior sub-region with dynamic ice surface conditions. RGB pixel values were scaled to two standard deviations for SWIR1, NIR, and Green spectral bands (Landsat ETM+ radiance saturated over snow). We selected 3x3 kilometer sub-regions with a clear field-of-view across a north south transect with stable ice, pressure cracks, floating ice, and open water. The black box represents the Chequamegon Bay ice surface retrieval sub-region. Grey and white boxes indicate Apostle Islands channel and deep-water retrieval sub-regions. The Landsat image strips shown here were cutouts from the full swath data to match the narrow 7 km Hyperion swath.

Graphic 2: EO-1 Hyperion, Landsat OLI, and Landsat ETM+ sub-pixel ice surface endmember fractions were retrieved with a constrained linear un-mixing model. Only results from the Apostle Islands channel are shown here. Spectral reflectance endmembers were derived from directional inland lake spectroscopic measurements of accumulated snow, snow ice, clear lake ice, and shallow water collected from the western Great Lakes region in February and March 2015. RGB image composites (NIR, Red, Green spectral bands) are scaled to two standard deviations. Sub-pixel endmember fractions and root-mean-squared-error (RMSE) are scaled to absolute minimum and maximum values. Black pixel regions indicate No Data and/or cloud/cloud shadow contamination. More work is required in the technical areas of instrument development, calibration/validation, and atmospheric correction when defining optical instrument and science requirements for snow, ice, and water.

Scientific significance, societal relevance, and relationships to future missions: Recent evidence from the published literature suggests that inland lakes may be warming at rates faster than land. This environmental change has large implications for seasonal freshwater ice concentrations, lake eutrophic processes, aquatic ecosystems, and increasing concentrations of potentially harmful algal blooms. This remote sensing work on freshwater ice using satellite Earth observations can inform how inland lakes have responded, are responding, and will respond to recent climatic changes, and then from a societal perspective, how these changes will impact rural economies, navigation and commerce, and availability of potable freshwater. This work uses current mid resolution NASA Earth observing missions to characterize current optical instrument capabilities for measuring lake accumulated snow, freshwater ice, and open water. Christopher J. Crawford will present this peer-reviewed study at the 23rd IAHR International Symposium on Ice in Ann Arbor, Michigan in late May 2016. Crawford will also present this study as a contribution to the spring HyspIRI mission data products workshop at NASA/GSFC in early June 2016. There is also potential for this work to inform SnowEx mission objectives for which Crawford is involved as a organizing team member.

30 Years of Change to the Antarctic Peninsula from Landsat (1986-2016)

Christopher A. Shuman, Cryospheric Sciences, NASA GSFC, UMBC JCET

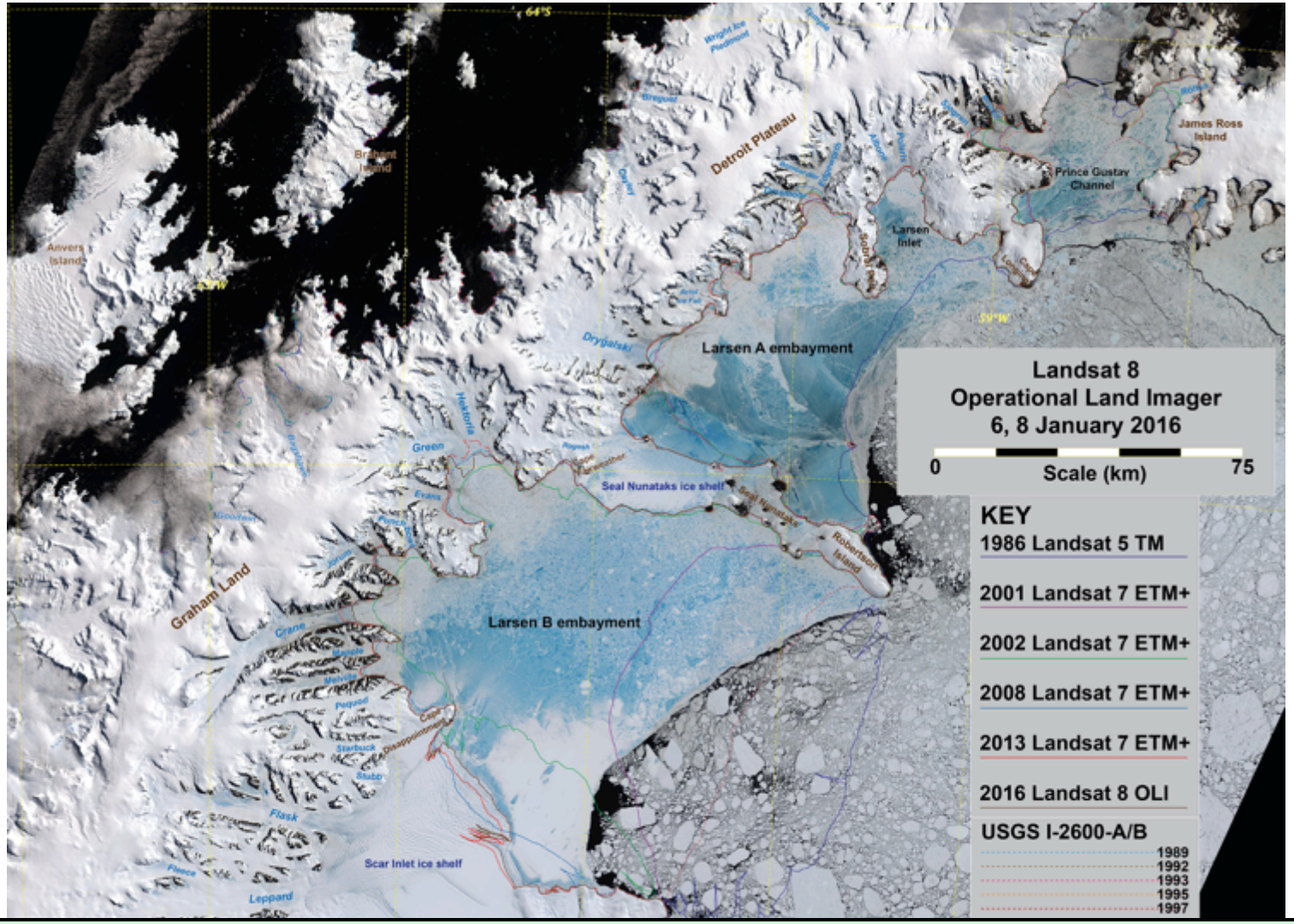

A Landsat 8 Operational Land Imager mosaic from January 2016 provides a backdrop to highlight 30 years of land ice changes in the northern Antarctic Peninsula. Sea ice in the embayments since 2011, shows a cover of blue melt water in the early austral summer.

Name: Christopher A. Shuman, Cryospheric Sciences, NASA GSFC and UMBC JCET
E-mail: cshuman@umbc.edu, christopher.a.shuman@nasa.gov
Phone: 301-614-5706

References:

Shuman, C.A., E. Berthier, and T.A. Scambos, (2016). Changes in the Seal Nunataks Ice Shelf Region from Imagery and Altimetry, submitted to Annals of Glaciology, in review.

Scambos, T.A., E. Berthier, T. Haran, C.A. Shuman, A.J. Cook, S.R.M. Ligtenberg, and J. Bohlander (2014). Detailed ice loss pattern in the northern Antarctic Peninsula: widespread decline driven by ice front retreats, *The Cryosphere*, 8, 2135-2145, doi: 10.5194/tc-8-2135-2014.

Berthier, E., T. A. Scambos, and C.A. Shuman (2012). Mass loss of Larsen B tributary glaciers (Antarctic Peninsula) unabated since 2002, *Geophysical Research Letters*, 39 (13), L13501. doi:10.1029/2012GL051755

Shuman, C.A., E. Berthier and T. Scambos, (2011). 2001-2009 elevation and mass losses in the Larsen A & B embayments, Antarctic Peninsula. *Journal of Glaciology*, 57(204), pp. 737-754, doi:10.3189/002214311797409811.

Scambos, T.A., E. Berthier and C.A. Shuman (2011). The triggering of sub-glacial lake drainage during the rapid glacier drawdown: Crane Glacier, Antarctic Peninsula. *Annals of Glaciology*, 52(59), pp. 74-82, doi:10.3189/172756411799096204.

Data Sources: Landsat 5, 7, and 8 data were used to create this time series of ice edge positions for the northern Antarctic Peninsula. Ice-edge data from two USGS publications (Ferrigno et al., 2006; 2008; http://pubs.usgs.gov/imap/2600/) were also integrated into the study. The support of Patricia Vornberger and Katherine Melocik was also important to the overall study.

Ferrigno, J.G., Cook, A.J., Foley, K.M., Williams, R.S., Jr., Swithinbank, Charles, Fox, A.J., Thomson, J.W., and Sievers, Jörn, (2006). Coastal-change and glaciological map of the Trinity Peninsula area and South Shetland Islands, Antarctica -- 1843–2001: U.S. Geological Survey Geologic Investigations Series Map I–2600–A, 1 map sheet, 32-p. text.

Ferrigno, J.G., Cook, A.J., Mathie, A.M., Williams, R.S., Jr., Swithinbank, Charles, Foley, K.M., Fox, A.J., Thomson, J.W., and Sievers, Jörn, (2008). Coastal-change and glaciological map of the Larsen Ice Shelf area, Antarctica: 1940–2005: U.S. Geological Survey Geologic Investigations Series Map I–2600–B, 1 map sheet, 28-p. text.

Technical Description of Figure: The Landsat 8 Operational Land Imager (OLI) scenes acquired in early 2016 enables the evolution of ice shelf and glacier front positions to be visualized over 30 years of change. Starting in 1986 with a Landsat 5 Thematic Mapper (TM) scene pair, and followed by Landsat 7 Enhanced Thematic Mapper + (ETM+) scene pairs in 2001, 2002, 2008, and 2013, the mapped ice edge positions show dramatic ice shelf losses in the late 1980s and early 1990s for the Larsen Inlet and Prince Gustav Channel Ice Shelves. These losses accelerated with major collapses to the Larsen A Ice Shelf and also the front of the Larsen B Ice Shelf beginning in 1995. By 2001, the Larsen B was in a precarious state with a unstable 'arch' across the ice shelf front. With additional melting from above and below, the major collapse (>3250 km^2 by late 2002) that was also captured by multiple EOS sensors separated the Larsen B into the Seal Nunataks and Scar Inlet shelf remnants with a large embayment. The glaciers that once fed all the shelf areas show distinct ice front retreats by 2008 and multiple studies (Scambos et al., 2011, 2014; Berthier et al., 2012; Shuman et al., 2011, 2016) show dramatic ice elevation decreases and continuing shelf losses to this part of the Antarctic Peninsula's ice cover. From the maximum retreat positions in ~2010 and with more persistent sea ice at least since March 2011, as tracked with MODIS imagery, several major glaciers (e.g. Crane, Green, Hektoria) have advanced several kilometers as has the crumbling and deeply rifted front of the Scar Inlet shelf remnant. The natural color, 4,3,2 band composite for the Landsat 8 mosaic allows the deep blue of melt water on glaciers, shelf ice, and broadly across the embayment's sea ice cover to be clearly seen.

Scientific significance, societal relevance, and relationships to future missions: The continuing observations from the Landsat sensor series of these areas of unmistakable climate change in the polar regions provides compelling visuals for the public, scientific colleagues, and policymakers.

Arctic Sea Ice Maximum and Minimum Extent 1979-2016

Walt Meier, Cryospheric Sciences, NASA GSFC

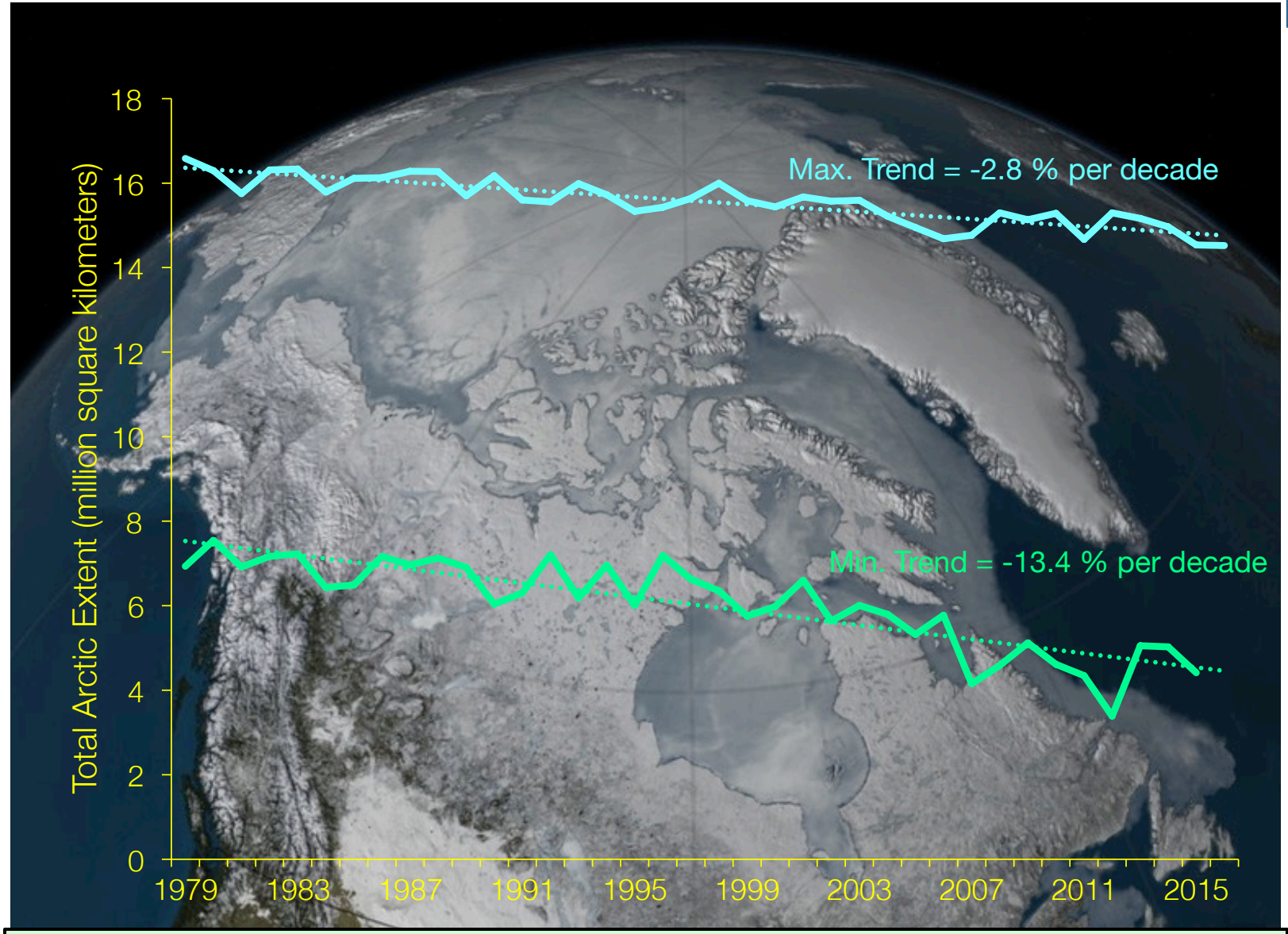

Arctic sea ice extent reached its annual maximum extent this year on March 25, 2016. This year's extent was the lowest extent in the satellite record. However, this does not necessarily portend a record summer minimum.

Name: Walt Meier, NASA/GSFC Cryospheric Sciences, NASA GSFC
Email: walt.meier@nasa.gov
Phone: 301-614-6572

References:
A joint announcement was made by NASA Goddard and the National Snow and Ice Data Center (NSIDC), Boulder, CO. The releases were published on NSIDC's Arctic Sea Ice News and Analysis web page and the NASA News Releases. Multimedia material was developed by NASA Goddard's Scientific Visualization Studio (SVS). NSIDC is a NASA Distributed Active Archive Center (DAAC).

NASA Release: http://www.nasa.gov/feature/goddard/2016/2016-arctic-sea-ice-wintertime-extent-hits-another-record-low
NSIDC Announcement: http://nsidc.org/news/newsroom/arctic-sets-yet-another-record-low-maximum-extent
NASA SVS Material: https://svs.gsfc.nasa.gov/cgi-bin/details.cgi?aid=4440

Data Sources:
Sea ice extent data are from the NASA Team algorithm, distributed by the National Snow and Ice Data Center Sea Ice Index (references below). The background image is the sea ice cover on 24 March 2016, the date of the maximum extent for the year, from the AMSR2 sensor on JAXA's GCOM-W1 satellite overlaid on the NASA Blue Marble; the image was produced by the NASA Goddard Scientific Visualization Studio (SVS). Trend is calculated relative to the 1979 trend value of the maximum and minimum extents. Total extent refers to the sum of all areas that have at least 15% concentration ice cover.

- Fetterer, F., K. Knowles, W. Meier, and M. Savoie. 2002, updated daily. *Sea Ice Index, Version 1*. Boulder, Colorado USA. NSIDC: National Snow and Ice Data Center. doi: http://dx.doi.org/10.7265/N5QJ7F7W.
- Cavalieri, D. J., C. L. Parkinson, P. Gloersen, and H. J. Zwally. 1996, updated yearly. *Sea Ice Concentrations from Nimbus-7 SMMR and DMSP SSM/I-SSMIS Passive Microwave Data, Version 1.* Jan 1979 – Dec 2014. Boulder, Colorado USA. NASA National Snow and Ice Data Center Distributed Active Archive Center. doi: http://dx.doi.org/10.5067/8GQ8LZQVL0VL.
- Maslanik, J. and J. Stroeve. 1999, updated daily. *Near-Real-Time DMSP SSMIS Daily Polar Gridded Sea Ice Concentrations, Version 1.* Jan 2015 – Mar 2016. Boulder, Colorado USA. NASA National Snow and Ice Data Center Distributed Active Archive Center. doi: http://dx.doi.org/10.5067/U8C09DWVX9LM.

Technical Description of Figure:
The figure shows the maximum extent (blue) for 1979 to 2016 and the minimum extent (green) for 1979 to 2015. The maximum and minimum extents are daily total area of ice with at least 15% concentration and are based on a 5-day trailing average of daily values (this is done to remove short-term noise due to satellite/algorithm errors and synoptic effects). A linear trend line is fit to both time series and relative trends are given in % per decade relative to the 1979 trend value. Background: 24 Mar 2016 Extent, from NASA Goddard Scientific Visualization Studio (SVS) and data from NASA Goddard and the National Snow and Ice Data Center (NSIDC)

Scientific significance, societal relevance, relationships to future missions: The Arctic sea ice is declining at a significant rate, most prominently in summer, but significant trends are also found in winter (maximum extent). The loss of sea ice has substantial implications for climate (more solar absorption by the larger ocean area during summer, potential effects on weather patterns), human activities in the Arctic (resource extraction, national security, indigenous culture), and ecology (polar bears, etc.). There is also evidence that ice is thinning, though data has historically been sparse. ICESat-2 will significantly increase our understanding of thickness and changes in the sea ice mass balance, provide a more complete picture of Arctic sea ice change, inform policymakers and other stakeholders in the future of the Arctic, and enhance predictive capabilities of models on seasonal to decadal time scales.

Physical Controls on the Distribution of Colored Dissolved Organic Matter in the Southern Ocean

C.E. Del Castillo, Ocean Ecology, NASA GSFC, S. Dwivedi, Department of Atmospheric and Ocean Sciences, University of Allahabad, INDIA and
T. W. N. Haine, Earth and Planetary Sciences, Johns Hopkins University

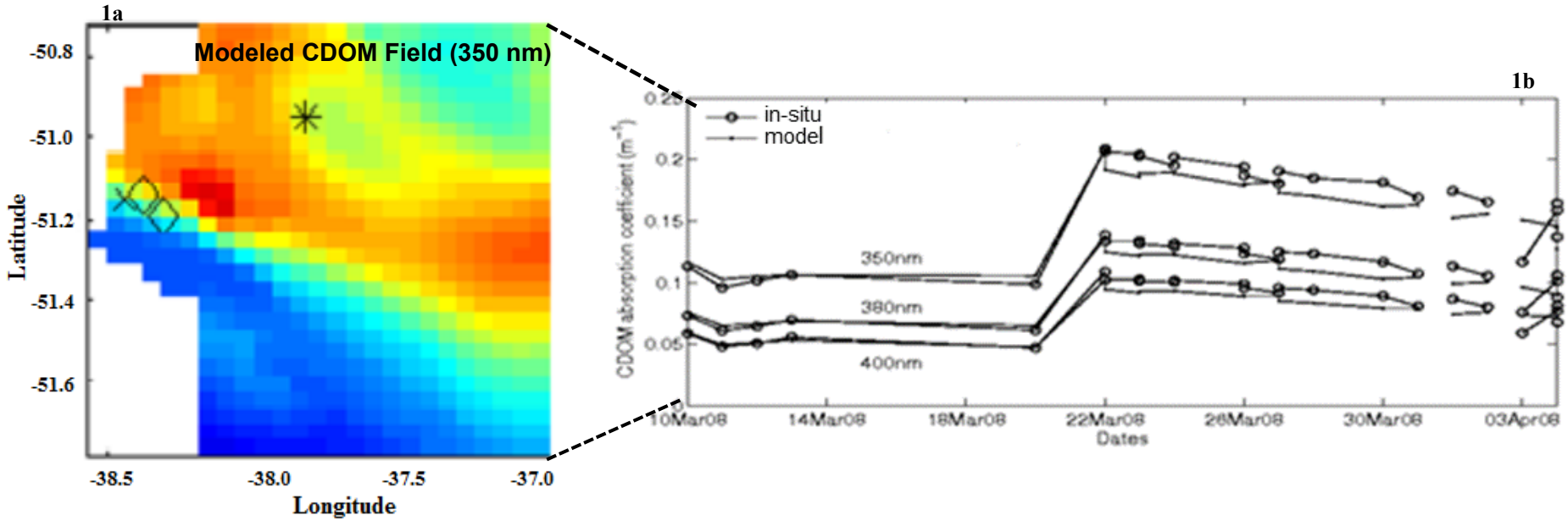

A 4-dimensional model with a photodegradation module recreated the spatial and temporal distribution of Colored Dissolved Organic Matter (CDOM) in the Southern Ocean GasEx site. Over periods of weeks, CDOM is controlled by mixing and photodegradation. Biological processes are negligible over this time scale.

Name: Carlos E. Del Castillo, Ocean Ecology, NASA GSFC
E-mail: Carlos.e.delcastillo@nasa.gov
Phone: 301-286-8787

References:

C.E. Del Castillo; Dwivedi S., and T.W.N. Haine,. In preparation. Physical controls on the distribution of CDOM in the Southern Ocean

Del Castillo, C.E., R.L. Miller. 2011. Horizontal and Vertical Distribution of Colored Dissolved Organic Carbon During the Southern Ocean GasEx Expedition. Journal of Geophysical Research -Oceans. VOL. 116, C00F07, doi:10.1029/2010JC006781, 2011

Dwivedi S., T.W.N. Haine, and C.E. Del Castillo. 2011. Ocean State Estimation in the Southern Ocean Gas Exchange Experiment Region Using 4DVAR. JGR-Oceans. 116, C00F02, doi:10.1029/2009JC005615, 2011

Data Sources: Absorption coefficient of CDOM from MODIS Aqua, Normalized Absolute Dynamic Topography, AVHRR SST, field data from the Southern Ocean Gas Exchange Experiment

Technical Description of Figures:
Graphic 1a: Spatial distribution of CDOM (ag 350 nm) in the Southern Ocean GasEx area based on an ocean state estimation with a photochemical sink. Figure 1b. Comparison between modeled and in-situ CDOM at three wavelengths. Samples were collected along the cruise track of the Southern Ocean GasEx. The model was initiated with CDOM data from vertical profiles on day one of the simulation.

Scientific significance, societal relevance, and relationships to future missions: We demonstrated that a sea estimation can be used to model CDOM distribution in the ocean. Comparison between modeled products and field data suggested that, over periods of weeks, CDOM distribution is controlled by mixing and photochemical processes, with negligible contribution from biological processes. This study also shows that data assimilation schemes can be successful in extending satellite products over areas contaminated by clouds and glint. The sea estimation models can be used to diagnose effect of physical and biogeochemical forcing controlling the distribution of optical components in ocean waters. This method is relevant to all ocean color missions.

Value of Available Global Soil Moisture Products for Agricultural Monitoring and Yield Prediction

Iliana E. Mladenova and John D. Bolten, Hydrological Sciences, NASA GSFC

Corn

Soybeans

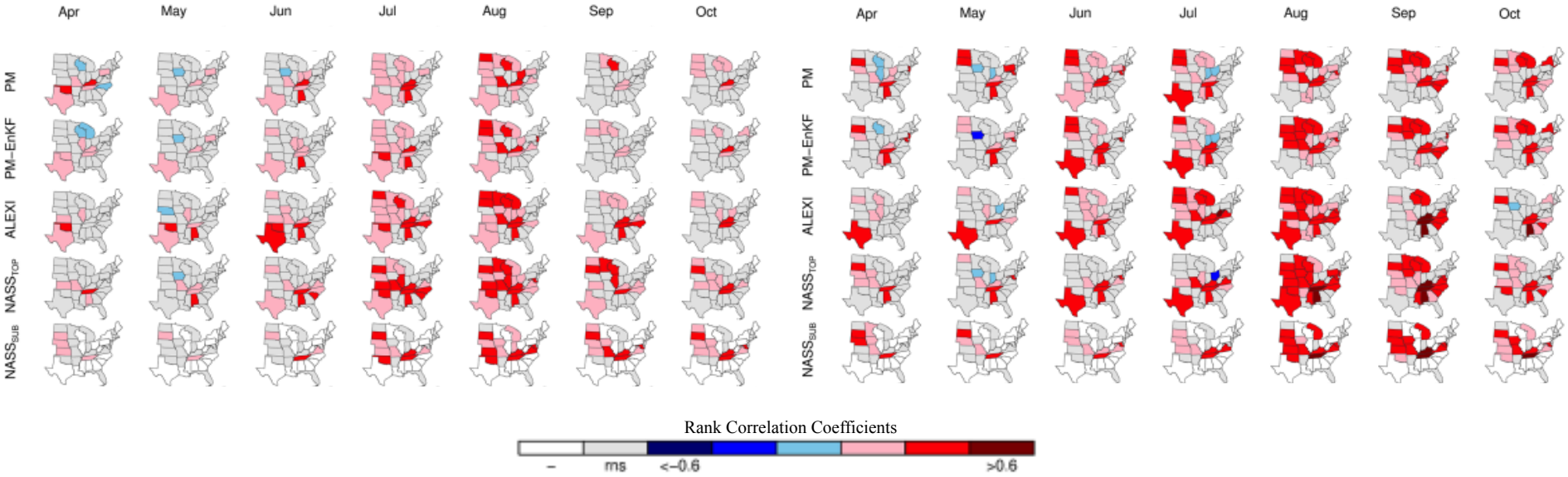

- PM stands for Palmer Model (hydrologic model used by USDA FAS) .
- PM-EnKF is an enhanced version of the PM generated by assimilating satellite-based soil moisture observations.
- ALEXI – soil moisture proxy estimated using an energy-based model that is driven by thermal imageries acquired from GOES.
- NASS – survey-based soil moisture product.

Satellite derived and numerically modeled soil moisture products provide timely and accurate information for monitoring and predicting global crop health and yields. Here, we show that merging satellite and modeled based products provides estimates of end of season crop yield comparable to more costly and labor intensive survey-based methods.

Name: Iliana E. Mladenova, Hydrological Sciences, NASA GSFC
E-mail: iliana.e.mladenova@nasa.gov
Phone: 301-614-6839

References:

Mladenova, I. E., J. D. Bolten, W. Crow and R. A. M. de Jeu (2016, April). "Value of Global Soil Moisture Products for Agricultural Monitoring," *EGU General Assembly,* Vol. 18, EGU2016-9762.

Mladenova, I. E., J. D. Bolten, W. T. Crow, M. C. Anderson, C. R. Hain, D. M. Johnson and R. Mueller. "Inter-comparison of Soil Moisture, Water Use and Vegetation Indices for Estimating Corn and Soybean Yields over the U.S.," *IEEE Journal of Selected Topics in Applied Earth Observations and Remote Sensing,* in review.

Mladenova, I. E., J. D. Bolten, W. Crow and R. A. M. de Jeu. "Assessing the Value of Global Satellite-based Soil Moisture and Vegetation Optical Depth Products for Vegetation Monitoring and Crop Productivity Estimation (working title)," *Remote Sensing of Environment,* in preparation.

Data Sources:

Modelled Products: Noah estimates obtained from the LDAS (Land Data Assimilation System) at NASA-GSFC; PM (Palmer Model) and PM-EnKF (Palmer Model – Ensemble Kalman Filter) obtained from NASA-GSFC; ALEXI ESI (Atmosphere-Land Exchange Inverse Evaporative Stress Index) estimates obtained from USDA ARS Hydrology and Remote Sensing office.
Survey Data: Soil moisture data and end-of season yield estimates obtained from the USDA NASS office.

Technical Description of Figures:

Figure: Depicts the results from the rank correlation analysis for corn (left) and soybean (right). Values were computed by inter-comparing the individual products against the end-of-season yield supplies that are estimated through the NASS survey program. Results show clear temporal evolution of the yield-index correlations during the growing season reaching maximum during the maximum plant water consumption periods.

Scientific significance, societal relevance, and relationships to future missions: Accurate, within-season information on factors limiting yield from optimal levels is of significant social benefit, providing essential information on market demand and supply and helping to identify food insecure areas. Current crop production forecasting systems require adequate knowledge of the available soil water in order to properly predict the impact of the in-season weather variations on the end-of-season crop production. Therefore, modeled and remote sensing-based products are an essential source of information which allow for the routine monitoring of moisture availability and vegetation development, particularly over remote areas where ground-based data are limited. This study helps to determine the value of available soil moisture, water use, and vegetation datasets for analyzing yield variability and to improve our understanding of the relationship between available water and crop yield and the strength and evolution of this relationship within the growing season.

Goddard Laser for Absolute Measurement of Radiance (GLAMR)

Joel McCorkel, Biospheric Sciences, NASA GSFC, Brendan McAndrew, Optics Branch, NASA GSFC,
Kurt Thome, Biospheric Sciences, NASA GSFC, and Jim Butler, Biospheric Sciences, NASA GSFC

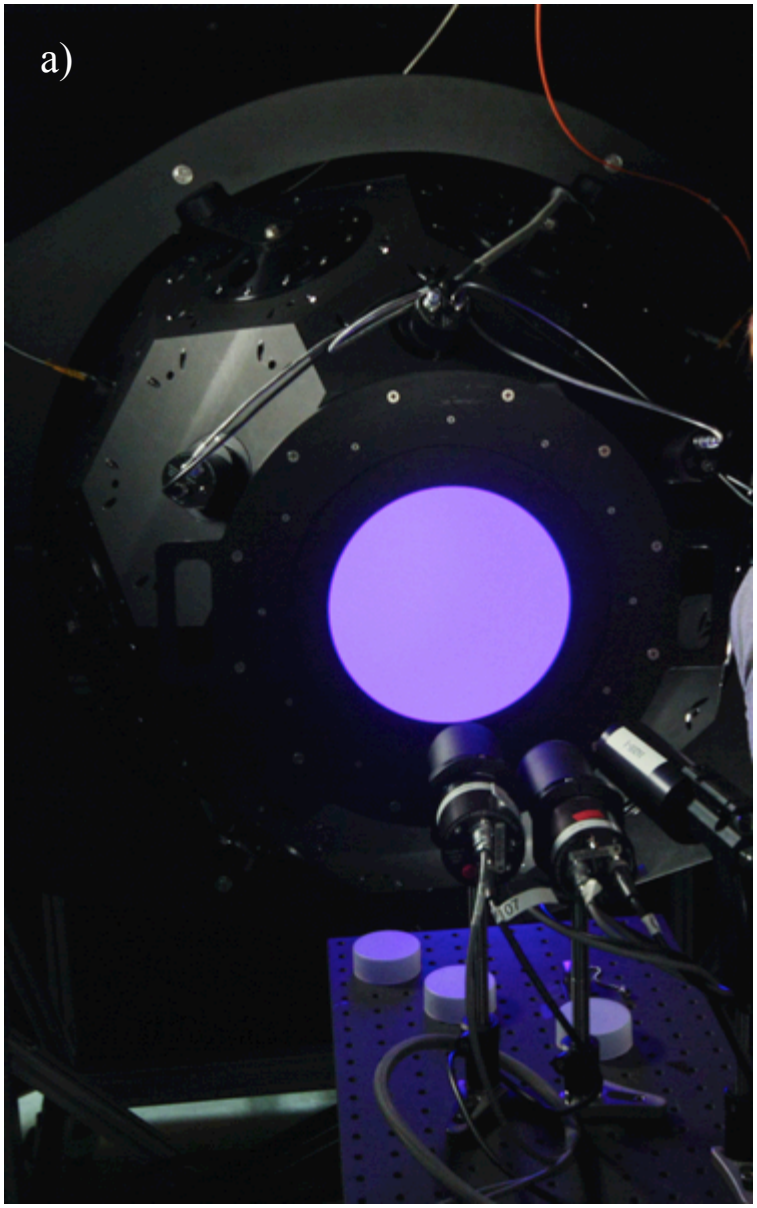

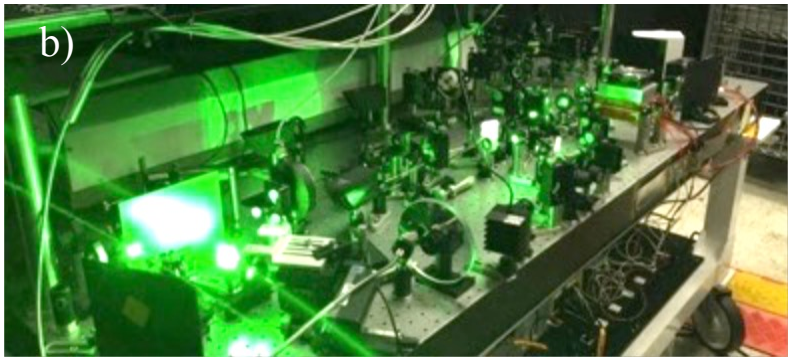

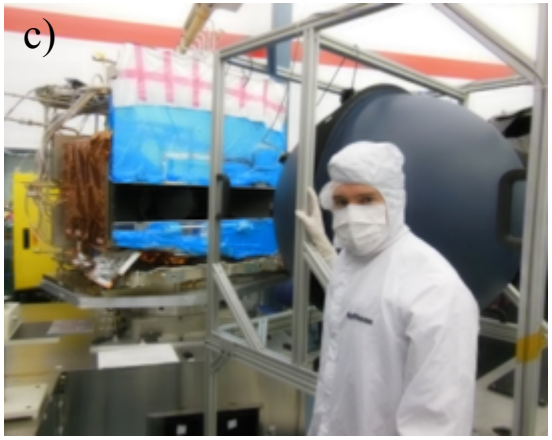

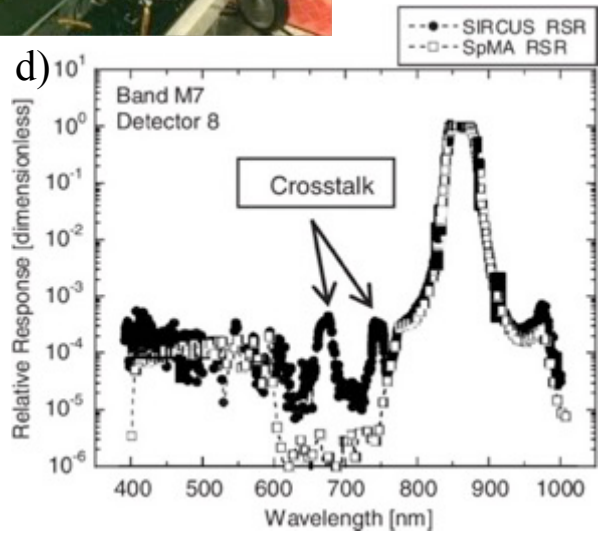

GLAMR is a tunable and high-powered laser system that provides an ideal light source for characterizing the spectral and radiometric response of an instrument. This pure signal allows decoupling of sensor features (e.g. linearity, crosstalk, scattered light) and orders of magnitude better absolute radiometric accuracies.

Name: Joel McCorkel, NASA/GSFC, Code 618
E-mail: joel.mccorkel@nasa.gov
Phone: 301-614-6675

Technical Description of Figures:
Graphic a: A photo of the integrating sphere that is coupled to the laser output of GLAMR via fiber optic, in this case GLAMR is tuned to 400 nm. The randomizing effect of the integrating sphere converts the Gaussian beam output from the fiber to a near-ideal source of radiance. In preparation for VIIRS characterization, the radiometers that are staring into the sphere in this photo are transferring SI-traceable radiometric knowledge to the monitors on the sphere.

Graphic b: GLAMR consists of several laser systems to achieve spectral tunability over the full solar reflective spectrum. This photo shows a portable optical table that hosts two LBO-based optical parametric oscillators that provide most of this spectrum.

Graphic c: This is a photo showing the experimental set up of the laser-based characterization of JPSS-1 VIIRS.

Graphic d: This plot provides an example of one of the sensor parameters that can be characterized with a laser-based calibration system, in this case cross talk.

Scientific significance, societal relevance, and relationships to future missions:
The Goddard Laser for Absolute Measurement of Radiance (GLAMR) provides an ideal light source for characterization of remote sensing instruments operating in the solar reflective spectrum: a monochromatic, extended source with SI traceability and accuracy more that ten times better than traditional calibration sources. Such a source allows better understanding of sensor features like nonlinearities, crosstalk, and scattered light which can be used to parameterize more sophisticated instrument models, the pathway for achieving accuracies to more quickly detect climate change and better decouple earth processes.

GLAMR will be used for to characterize the spectral and radiometric response of JPSS-2 VIIRS in summer 2016 in its first demonstration with a satellite instrument. Previous VIIRS sensors currently onboard Suomi NPP and JPSS-1 have been characterized by a similar laser system by NIST. Since this time NIST and NASA have been collaborating to transfer the methodology and technology for more operational use at GSFC. Currently, projects including JPSS-3/4 VIIRS, Landsat 9 OLI-2, PACE-OCI, and CLARREO Pathfinder have GLAMR as required activity of their prelaunch calibration plans.